11th International Conference on Fracture Mechanics of Concrete and Concrete Structures
FraMCoS-11
J. M. Chandra Kishen, A. Ramaswamy, S. Ray and R. Vidyasagar (Eds)
https://doi.org/10.21012/FC11.092366

CRACKING BEHAVIOUR UNDER CREEP IN STRAIN-HARDENING CEMENTITIOUS COMPOSITES (SHCC) APPLIED AS A PROTECTIVE LAYER ON REINFORCED CONCRETE FLEXURAL ELEMENTS

K. A. SHAN D. RATNAYAKE[*†], CHRISTOPHER K. Y. LEUNG[†]

[†]The Hong Kong University of Science and Technology, Hong Kong SAR, PR China
e-mail: kasdr@connect.ust.hk, ckleung@ust.hk

Key words: strain-hardening cementitious composites, cracking, creep, durability

Abstract: Strain-hardening cementitious composites (SHCC) have gained attention as a material capable of significantly enhancing the durability of infrastructure owing to their exceptional ductility and ability to effectively self-control cracking, surpassing conventional concrete in such aspects. These features play a key role in preventing the exposure of steel reinforcement to deleterious substances. However, long-term loading tests involving SHCC subjected to a constant stress have highlighted the potential growth of cracks to unacceptably large sizes, compromising durability. Such results may be an over-estimation for field conditions, where stress redistribution in the structural system will govern the stress-strain behaviour of SHCC with time. In this study, a reinforced concrete beam, with a SHCC layer applied on its tension face (mimicking a typical case where SHCC is used as a protective layer of a structural element) was subjected to a 4-point bending arrangement. The beam was loaded to 57.5% of its failure load and maintained at this level for 6 months, while strains and crack widths were continuously monitored. Results indicated the occurrence of cracks up to 65 µm initially, with the average crack width increasing by 28 µm over the test duration, indicating the crack widths were still within an acceptable range by the end of the test. Notably, the average crack widths observed during the long-term loading test remained within range of the quasistatic crack widths at corresponding strain values.

1 INTRODUCTION

Durability of reinforced concrete (R/C) structural elements have long been known to go hand in hand with its extent of cracking, as surface cracks can facilitate the penetration of water and chemicals [1, 2], to induce concrete degradation and corrosion of steel rebar. In the last several decades, as a material having the ability of self-controlling cracks to fine widths with little effect on water/chemical transport properties, strain-hardening cementitious composite (SHCC) has become popular in increasing the resiliency and durability of structures, potentially prolonging their design life [3, 4]. Tension and flexural tests show that cracks in SHCC can indeed be engineered to fall well below the 150-200 µm [5-7] service limit stipulated in R/C design codes [8] for severe environments.

Despite the attractive ductility and crack-control properties, it is often overlooked that such performances were observed under short term, or quasistatic loading regimes. In real structures where the SHCC is under load indefinitely, the creep effects come into play, where the crack expands, possibly overstepping on the limits in guidelines. Previous studies have already highlighted this unfavourable phenomenon, where in extreme cases, sub 100 µm cracks at the end of quasi-static loading reach in excess of 500 µm within two weeks of sustained constant loading [9]. At first glance, the crack

formation and widening of SHCC in the long-term [10, 11] does not seem conducive to the use of SHCC as a material in improving durability and longevity of structures.

However, due consideration must be also given to the actual conditions found in the field. To improve durability performance of R/C members, SHCC can be used as permanent formwork [12] or sprayed/cast surface layer serving as part of the concrete cover to act as a barrier to water/chemical penetration. Under such a condition, the SHCC element would not be subject to a constant loading as represented by constant loading creep tests, as stress redistribution in the system governs the stress and strain history of the SHCC and the R/C member. Therefore, the SHCC layer is not subject to a constant load, rather a hybrid form of relaxation. The cracking behaviour of SHCC in an exclusive load sharing system between a reinforcement bar and SHCC was investigated in the authors' previous study [13], where the crack widths increased only by 10 μm on average.

The current study attempts to simulate the cracking behaviour in a practical scenario where a protective SHCC layer is applied on a R/C beam. While the beam was loaded in a 4-point bending arrangement and is itself under a sustained constant load, the central pure bending region had a layer of SHCC at the tension face together with steel reinforcements inside to facilitating stress redistribution. The development of cracking was studied for a period of 4500 hours to better understand the behaviour of cracking in SHCC under creep conditions, in a more practically inclusive perspective. Implications to the durability design of R/C members with SHCC on the surface are also discussed.

2 EXPERIMENTAL PROGRAM

2.1 Materials and specimen preparation

To minimise the change of mechanical and chemical properties of the SHCC with time after starting the creep test, a high-strength SHCC having sufficient tensile strain capacity (>2%), reaching 85% its 90d compressive strength at 14 days, developed by Chen et al. [14] (shown in Table 1) was adopted for the study.

The cement used in the experiment was CEM I Class 52.5N Hong Kong Green Island ordinary Portland cement which contains at least 95% ground clinker. Silica fume used was Elkem™ 920U and silica sand (Mesh 80-120) was used as fine aggregate for SHCC. A high range water reducing superplasticiser, PCA-I from Subote™, was used to control the workability of the mixes. Quantaflex™ Polyethylene (PE) fibres were used to produce SHCC. SHCC specimens were prepared in a Hobart A200 mixer. In addition to these materials, commercially available river sand sieved through 5 mm sieve and 10 mm crushed aggregate was used as fine and coarse aggregate to produce C45 concrete in a pan mixer.

3 dog bone shaped specimens with 13 mm x 30 mm area at the neck and 3 coupon specimens with a 15 mm x 50 mm area were cast for tension tests of SHCC. 40 mm and 100 mm cubes were cast to determine compressive strength of SHCC and concrete respectively. Specimens were demoulded between 48-72 hours due to the delayed setting brought on by the high SP dosage and cured at a temperature of 23 ± 2 °C and relative humidity of 95 ± 5% until 14 days from date of casting. A 28-day curing period was adopted for concrete.

The simulation of a protective SHCC layer on concrete subject to creep deformation was achieved by placing a 15 mm thick SHCC layer on a 1.7 m × 0.1 m × 0.2 m reinforced concrete (R/C) beam along the central span. The SHCC layer was cast on the beam 14 days after the R/C beam cast and cured. The specimen was then cured further until 14 days of casting SHCC. Two such specimens were prepared – one for a quasistatic test to failure and the other for the long-term test. The concrete was reinforced by two 10 mm Ø high yield steel bars for tension (with a 100mm anchorage at each end) and two 10 mm Ø high yield steel bars for compression. Stirrups of 6 mm Ø mild steel at 125 mm spacing provided shear reinforcement. A cover of 12 mm was provided on all sides. The 15 mm SHCC layer

placed covering the central 600 mm region (of the tension face of the beam) consisted of 3 consecutive dog-bone shaped segments (or zones) (with a 15 mm × 50 mm narrowed section), each having a lifting hook anchored through the SHCC layer into the concrete at the widest sections of the layer as shown in Figure 1. To concentrate most of the strain and cracks to the narrower sections, the 80 mm gauge length of each was debonded from the concrete surface using a polythene sheet on the concrete-SHCC interface prior to casting the SHCC layer.

Table 1: Mass proportions for SHCC

Component	SHCC	Concrete
Cement	0.80	1.00
Silica fume	0.20	-
Silica sand (80-120 mesh)	0.50	-
River sand 5mm	-	1.88
10 mm aggregate	-	1.47
Water	0.18	0.44
Superplasticizer	0.033	0.009
Fibre % (by volume)	2.20	-

2.2 Test setup

To characterise the quasistatic tensile properties of SHCC, the specimen was clamped at the two ends in a servohydralic MTS machine and tested under a displacement rate of 0.3 mm per minute until failure. Two linear variable differential transformers (LVDT) were used to capture the deformation in the gauge length (80 mm for dog bone, 175 mm for coupon specimens). The corresponding strain value was taken by averaging the LVDT data. A Canon EOS 6D Mark II camera was used to capture the lateral surface of the specimen every 20 seconds during testing. 40 mm cubes were tested in compression at 0.625 MPa/s.

For the creep test specimen, a uniform moment was imposed throughout the midspan, a 4-point bending arrangement was employed, with a middle span of 600 mm and loading points 100 mm from each end of the beam. To maintain a constant load at each end, hydraulic cylinders fitted with a valve for maintaining pressure was used. The cylinders were fixed to a load cell and rested on a 100 mm strip of steel pasted onto the top surface of the beam at the loading point. Manual hydraulic pumps were used for stroke control of the cylinder. The schematic of the loading system and its components are shown in Figure 2. A single LVDT placed on the surface of each SHCC segment at its wide section measured the deformation within the gauge length. Since it was expected that the cracks would be concentrated in the middle 80 mm gauge length of the SHCC with reduced area, the LVDT would predominantly capture the deformation in the gauge length in addition to the elastic deformation in the outer 35 mm on each side. As the elastic strain is negligible compared to strains arising due to crack formation, it was not considered.

The first beam specimen was loaded quasistatically to failure. Crack patterns of each segment were captured at every 1 kN increment of loading.

The second beam specimen was quasistatically loaded to 57.5% (analogous to a service load) of the first specimen's failure load, and a load of 57.5 ± 3.0% was maintained for 4500 hours at 23 ± 2 ˚C and relative humidity 60% ± 10%. When the load in hydraulic cylinders dropped due to the creep deformation of concrete and SHCC, the load was increased by tightening the nuts on the top plate, thus moving the top plate downward. During this period, a USB microscope (having a resolution of ~0.5 µm/pixel) was periodically used to capture images of each crack at specific locations to calculate crack widths. A line was drawn across the surface cracks to mark and identify the monitoring region of each.

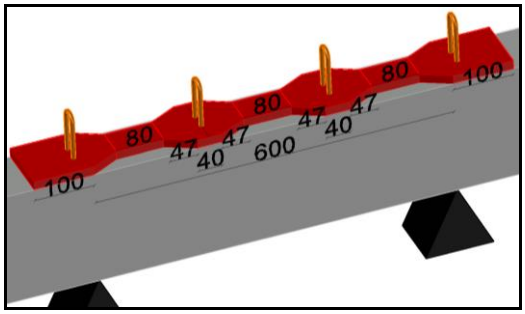

Figure 1: Conventional concrete beam with SHCC layer (dimensions in mm)

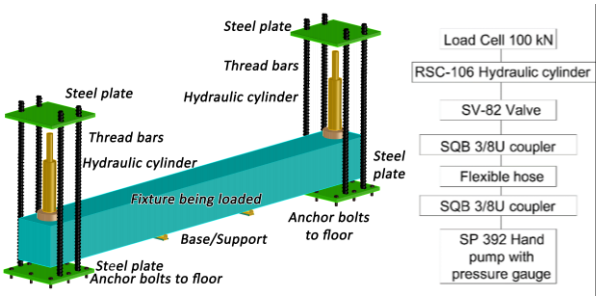

Figure 2: Schematic of loading system for the fixture

3 RESULTS AND DISCUSSIONS

3.1 Quasistatic characterisation tests

The 14-day tensile and compressive properties of the SHCC are summarized in Table 2 and the tensile stress-strain curves are shown in Figure 3. The average tensile strain capacity exceeded 2%. Average crack width on the dog bone and coupon specimen at 1% strain was ~52 µm and ~62 µm respectively.

Table 2: Mechanical properties of SHCC

Specimen	Tensile strength (MPa)	Tensile strain capacity (%)	Compressive strength (MPa)
13 mm dog bone	7.6(1.3)	2.4(1.1)	115(15)
15 mm coupon	7.8(0.7)	2.1(1.3)	
Concrete	-	-	59(1)

**standard deviation mentioned in brackets*

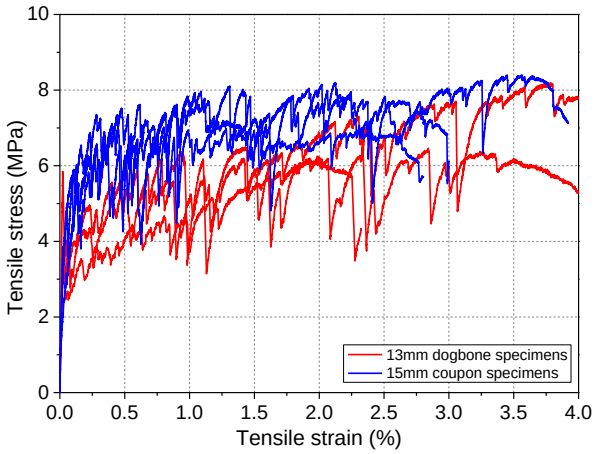

Figure 3: Tensile stress-strain curves for 13 mm dog bone and 15 mm coupon specimens

3.2 Creep test

A shear failure at 35 kN was observed in the first specimen which was quasistatically loaded to failure. The photographs of crack patterns at failure and the development of strain within each segment of the SHCC layer are shown in Figure 4 and Figure 5 respectively. Tensile strains between 1.0-1.4% were exhibited in each segment at failure and multiple cracks were observed albeit a majority being concentrated near ends of the gauge length.

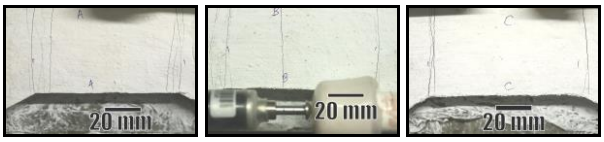

(a) (b) (c)

Figure 4: Crack pattern of zone (a) A, (b) B and (c) C of the SHCC layer at failure

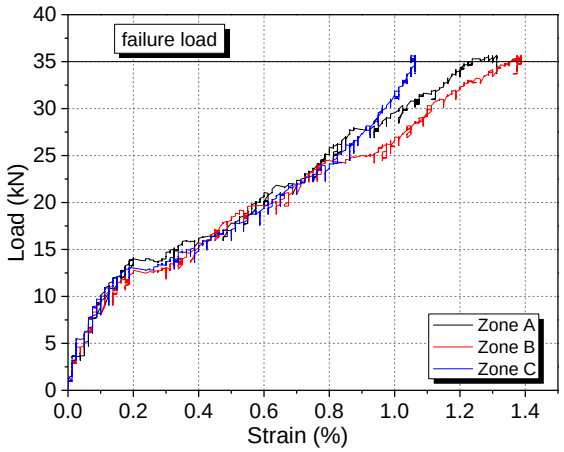

Figure 5: Strain development in each section of the SHCC layer with load

The second specimen was loaded to 20 kN quasistatically and this load was maintained within 1 kN for the sustained load phase. The surface cracking pattern in each zone just after reaching the target load is shown in Figure 6. A new crack was formed in zone B after 27 hours, and the branching of a crack was observed in one of the cracks in zone C within 24 hours.

Figure 7 shows the variation of the load and strain during the testing period. The change of individual crack widths (in the sustained loading phase) with time and strain is shown in Figure 8 and Figure 9 respectively. Due to the

discrete random nature of cracking locations on the top surface of the R/C beam, the deformation in the three zones were not the same at any given instance. An initial reduction in the crack width was observed in one of the cracks in zone C, which corresponded to the branching of the existing crack, causing the initial crack to narrow.

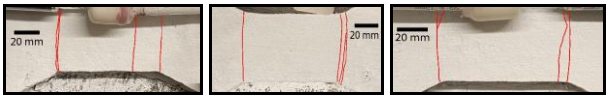

(a) (b) (c)

Figure 6: The surface crack pattern on reaching target load in zone (a) A (b) B and (c) C (traced in red for clarity)

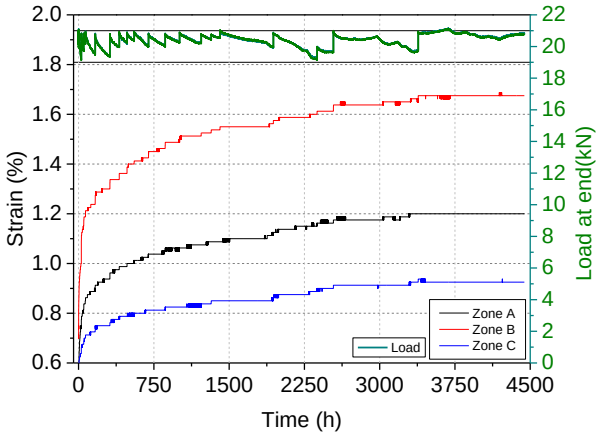

Figure 7: Variation of load and strain in each zone for the duration of the test

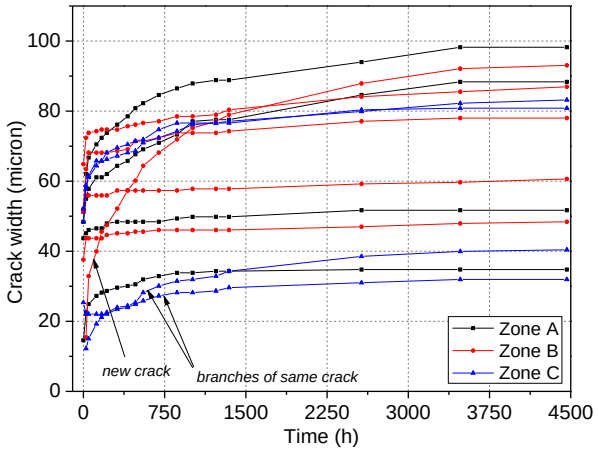

(a)

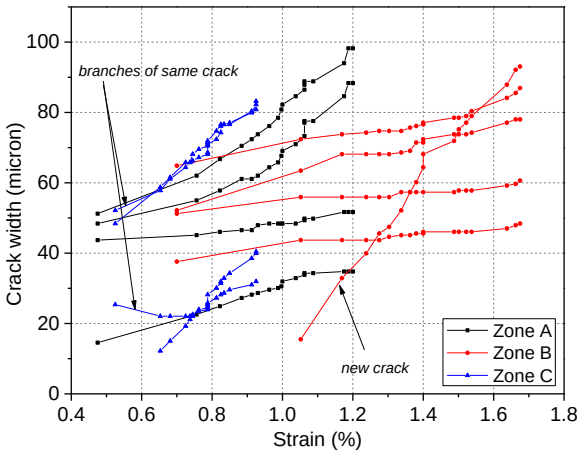

(b)

Figure 8: Variation of individual cracks with (a) time and (b) strain

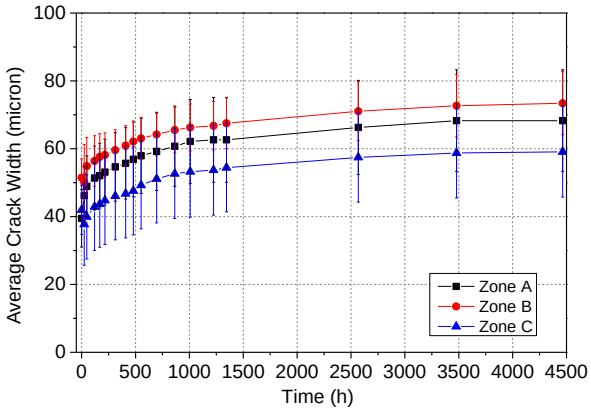

(a)

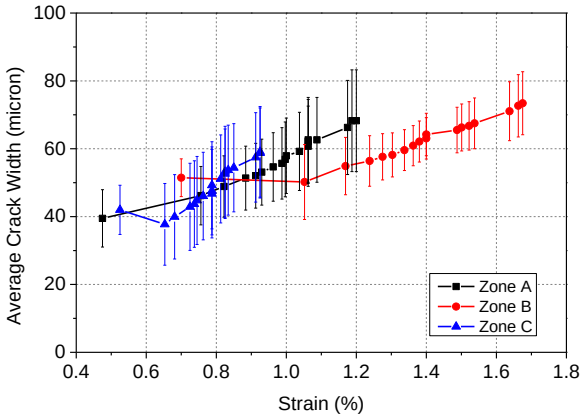

(b)

Figure 9: Variation of average cracks with (a) time and (b) strain

Cracks up to 65 µm width were observed at the start of the sustained loading phase. An average crack width increase of 25-30 µm in all zones is observed within 4500 hours, with the majority (21 µm on average) of the deformation taking place within the first 1000 hours. By the end of 4500 hours, all crack

widths were still lower than 100 µm, with the average crack width being below 80 µm, as shown in Figure 8. It is observed that from the 13 cracks under study, 10 of the cracks expanded less than 100% of its initial width at 4500 hours. Of the 3 outliers, only one of them were present at the end of the quasistatic loading phase, while the remaining cracks were either formed after 27 hours, or as a branch of an existing crack. While a branch was formed from an existing crack, the opening of the main crack decreased, hence the reason one crack in zone C is observed to have an initial reduction in width.

An example of a crack expansion is shown in Figure 10. A roughly linear relationship between each crack width change with strain was observed (see Figure 11). The relationship between the average crack width and strain increment shows a very similar linear correlation in all 3 zones (shown in the same figure). This could be particularly because there was no new crack forming after the first 27 hours, whereby the increase in strain is accommodated by the proportionate widening of the existing cracks.

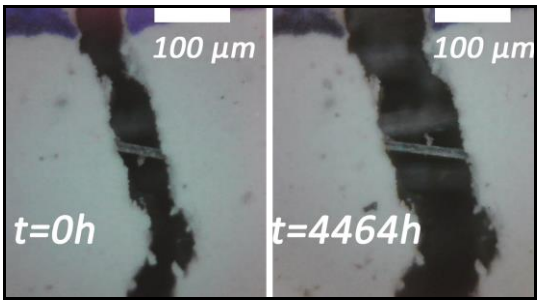

Figure 10: Crack widening as observed using the USB microscope

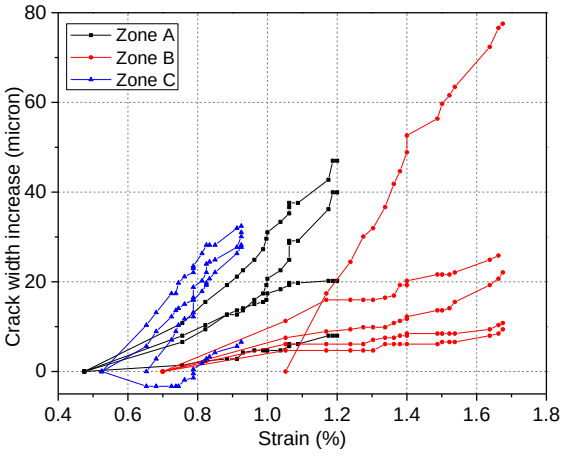

(a)

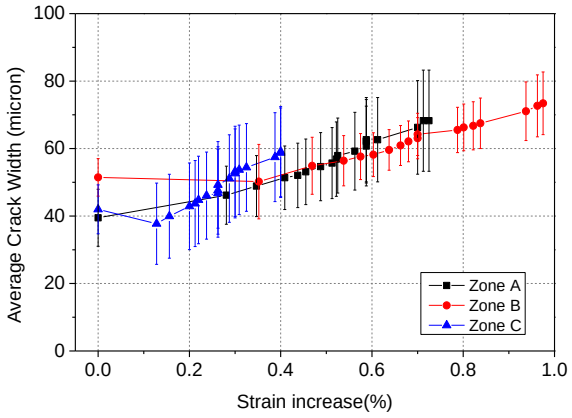

(b)

Figure 11: Variation of (a) individual crack width increase with strain and (b) average crack widths with strain increase

The average crack width development with strain in restrained creep also follows very closely that exhibited by the quasistatically tested specimens in direct tension (see Figure 12). However, it is important to distinguish the underlying factors driving the average crack width in each case. For the quasistatically tested specimens, new cracks are being formed as the strain increases, with variation within the material (flaw size distribution, non-uniform fibre distribution, increased elastic deformation of bridging fibres at higher stresses) leading to the overall widening of cracks. In contrast, the average crack width increases in restrained creep mostly due to widening of existing cracks, driven by the creep of the fibre-matrix interface, creep deformation of the SHCC matrix, creep deformation of the concrete in compression and rebar debonding with time.

As the driving factors in each case are different, the average crack width development in restrained creep may not always be within the envelope of the quasistatic crack width development (with strain). As such, it will be worthwhile to compare the most critical case of crack width development in restrained creep with the quasistatic crack width development. In this case, the member depth under study (200 mm) comes across as being more critical for the analysis, as neutral axis shifts (caused by creep in compression concrete etc.) have a more pronounced impact on the concrete tension surface, as compared to flexural

members having larger depths.

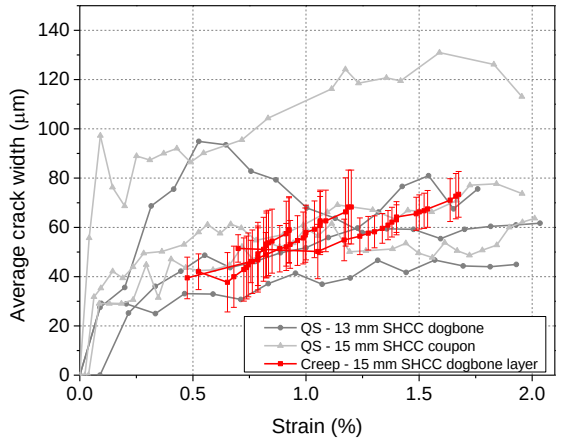

Figure 12: Comparison of SHCC average crack width development in restrained creep vs quasistatic testing

4 CONCLUSIONS

When the flexural specimen with the SHCC layer (with 3 dog-bone shaped segments) was tested to failure quasistatically, the tension strains in each zone reached 1.0-1.4%. The following findings can be highlighted:

1) Loading a specimen to 57.5% of the failure load induced a strain between 0.4-0.7% in each zone of the SHCC and maintaining ±3.0% of failure load level, for 4500 hours led to an average crack width increase of 28 μm. This is considerably less than the increases previously reported on creep tests where SHCC was at a constant stress.
2) All cracks were below 100 μm at the end of the sustained load period. In this case, the final crack widths remain under the crack width limits stipulated in the design codes [8]. As the formation of additional cracks post quasistatic loading phase was not pronounced, the expansion of existing cracks accommodated the increase in strain, thereby a roughly linear relationship was observed between the strain increment and average crack widths in each zone.
3) Although the existing cracks were expanding with time, the average crack widths in the SHCC layer throughout the sustained load period was still within the typical crack widths observed during quasistatic direct tension tests at the relevant strain level.

This investigation provides insights into the behaviour of SHCC under sustained loading conditions, offering a more realistic assessment of its performance under practical conditions.

REFERENCES

[1] K. Wang, D. C. Jansen, S. P. Shah, and A. F. Karr, "Permeability Study of Cracked Concrete," *Materials and Structures*, vol. 32, pp. 370–376, 1999.

[2] P. K. Mehta and R. W. Burrows, "Building durable structures in the 21st century," *Concrete international*, vol. 23, no. 3, pp. 57-63, 2001.

[3] V. C. Li, "Integrated structures and materials design," *Materials and Structures*, vol. 40, no. 4, pp. 387-396, 2007.

[4] V. C. Li, H. Horii, P. Kabele, T. Kanda, and Y. M. Lim, "Repair and retrofit with engineered cementitious composites," *Engineering Fracture Mechanics*, vol. 65, no. 2, pp. 317-334, 2000.

[5] M. D. Lepech and V. C. Li, "Water permeability of engineered cementitious composites," *Cement and Concrete Composites*, vol. 31, no. 10, pp. 744-753, 2009.

[6] M. Sahmaran, M. Li, and V. C. Li, "Transport Properties of Engineered Cementitious Composites under Chloride Exposure," *ACI Materials Journal*, vol. 104, no. 6, pp. 604-611, 2007.

[7] M. Maalej and V. C. Li, "Introduction of Strain-Hardening Engineered Cementitious Composites in Design of Reinforced Concrete Flexural Members for Improved Durability," *ACI Structural Journal*, vol. 92, no. 2, pp. 167–176, 1995.

[8] *Code of Practice for Structural Use of Concrete. B.D, HKSAR*, 2013.

[9] W. P. Boshoff, "Cracking Behavior of Strain-Hardening Cement-Based Composites Subjected to Sustained

Tensile Loading," *ACI Materials Journal,* vol. 111, no. 5, 2014.

[10] W. P. Boshoff and G. P. A. G. van Zijl, "Time-dependent response of ECC: Characterisation of creep and rate dependence," *Cement and Concrete Research,* vol. 37, no. 5, pp. 725-734, 2007.

[11] W. P. Boshoff, V. Mechtcherine, and G. P. A. G. van Zijl, "Characterising the time-dependant behaviour on the single fibre level of SHCC: Part 1: Mechanism of fibre pull-out creep," *Cement and Concrete Research,* vol. 39, no. 9, pp. 779-786, 2009.

[12] C. K. Y. Leung and Q. Cao, "Development of pseudo-ductile permanent formwork for durable concrete structures," *Materials and Structures,* vol. 43, no. 7, pp. 993-1007, 2010.

[13] K. A. S. D. Ratnayake, K. W. Li, and C. K. Y. Leung, "Cracking Behaviour of Strain-Hardening Cementitious Composites (SHCC) Under Practical Creep Conditions," in *Strain Hardening Cementitious Composites SHCC5*, Japan, M. Kunieda, T. Kanakubo, T. Kanda, and K. Kobayashi, Eds., 2023: Springer International Publishing, pp. 167-177,

[14] Y. Chen, J. Yu, and C. K. Y. Leung, "Use of high strength Strain-Hardening Cementitious Composites for flexural repair of concrete structures with significant steel corrosion," *Construction and Building Materials,* vol. 167, pp. 325-337, 2018.